

TRACE METAL ANOMALIES IN SOILS AND SEDIMENTS OF THE MOANDA-BANANA COASTAL AREA (CONGO COASTAL BASIN): RELATIVE ROLES OF ANTHROPOGENIC PROCESSES AND DEEP GEOGENIC CONTROLS

Yves Bolokole Mpehenzale ¹ , Crispin Kyela Mulaji ² , Emanuel Kazinguvu Atibu ³ , John Pote Wembonyama ³ , Dominique Wetshondo Osomba ³

¹ Exploration-Production Department, Faculty of Oil, Gas and Renewable Energies, University of Kinshasa, D.R. Congo

² Department of Chemistry and Industry, University of Kinshasa, D.R. Congo

³ Geosciences Department, Faculty of Science and Technology, University of Kinshasa, D.R. Congo

* Email (corresponding author): ybolokole2@gmail.com

DOI: 10.51865/JPGT.2026.01.04

ABSTRACT

This study investigates the controls governing the spatial distribution of trace metals (TMs) in soils and coastal sediments of the Moanda-Banana sector within the Congo Coastal Basin. The objective is to discriminate the relative roles of near-surface sedimentary processes and deeper geogenic influences in the development of metal anomalies within an active Atlantic margin context. Eighteen samples were collected along an ~8 km coastal transect during the 2025 dry season and analyzed using ICP-MS and AMA-254. The geochemical dataset was evaluated through enrichment and contamination indices (EF, Igeo, CF, DC and PLI), ecological risk factors (Eri and RI), multivariate statistics, and residual Bouguer gravity data.

Physico-chemical parameters show strong spatial contrasts between the estuarine domain of Moanda and the sandy environments of Banana. Fine estuarine sediments display high water contents (up to 76.9%) and total organic matter reaching 28.9%, whereas Banana soils are predominantly sandy (>80%). The highest metal concentrations occur at station M0S2, where Zn, Pb and Cu reach 412.6, 196.7 and 84.2 mg·kg⁻¹, respectively, indicating localized enrichment in fine-grained deposits. Zinc frequently exceeds the SQG guideline (123 mg·kg⁻¹) and locally approaches the PEL threshold (315 mg·kg⁻¹), while Pb surpasses the PEL value (91 mg·kg⁻¹) at stations M0S2 and M0S3.

At the regional scale, geochemical indices indicate predominantly low-to-moderate contamination despite localized enrichments, particularly for Pb and Zn. Principal Component Analysis explains 88.91% of total variance (F1=74.73%; F2=14.19%) and reveals a coherent Cu-Zn-Pb association mainly controlled by surficial sedimentary conditions. The overall ecological risk remains limited, although Hg and Cd represent the main local contributors. Residual Bouguer anomalies (- 0.69 to +1.97 mGal) indicate basement heterogeneity and show partial spatial correspondence with surface geochemical patterns. This spatial relationship is compatible with a possible halokinetic structural influence but does not demonstrate direct deep metal transfer. Overall, trace metal distribution in the Moanda-Banana coastal zone is dominantly controlled by surficial sedimentary processes, while deep geogenic influences remain secondary and locally plausible.

Keywords: trace metals, coastal geochemistry, enrichment factor, residual gravimetry, Congo Coastal Basin, estuarine sediments

INTRODUCTION

The Moanda-Banana coastal fringe, located at the westernmost extremity of the Democratic Republic of Congo, constitutes a key sector of the Congo Coastal Basin. This coastal domain forms an active interface between the continental margin, the Congo River estuary, and the Atlantic Ocean, where estuarine dynamics, port activities, and petroleum operations coexist (Figure 1). Recent studies have shown that coastal zones influenced by petroleum infrastructure may experience localized trace metal enrichment, although the magnitude of this impact remains highly site-specific [9],[10]. Owing to this superposition of natural and anthropogenic influences, the Moanda-Banana shoreline represents an environment particularly sensitive to the accumulation of trace metals (TMs), whose spatial distribution commonly reflects the interaction of multiple controlling processes [2],[4]

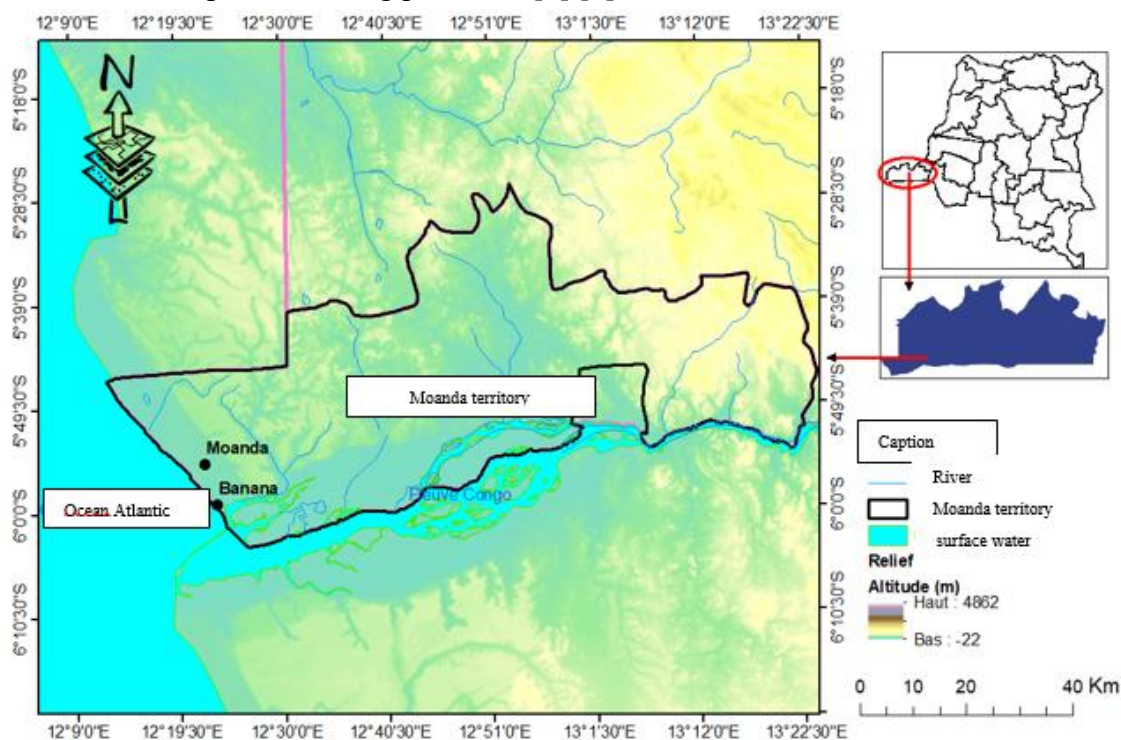


Figure 1. Location of the study area in the Congo Coastal Basin.

In coastal environments, the behavior of trace metals is generally governed by lithological inheritance, local physicochemical conditions, and anthropogenic inputs [12],[13]. However, in sedimentary basins affected by salt tectonics, deep geogenic controls particularly those related to halokinetic structures and fluid circulation may also influence surface metal enrichments and complicate their environmental interpretation [23],[24]. Within the Congo Coastal Basin, most previous investigations have primarily focused on anthropogenic contamination [4],[9],[18], whereas integrated approaches combining environmental geochemistry with geophysical constraints remain scarce.

As a consequence, the relative contribution of surficial sedimentary processes versus deep geogenic influences in controlling metal anomalies in the Moanda-Banana sector remains insufficiently constrained. This knowledge gap limits both the environmental assessment of metal contamination and the broader understanding of basin-scale controls on surface geochemical patterns.

Within this context, the present study investigates the spatial distribution of trace metals in soils and coastal sediments of the Moanda-Banana area using an integrated geochemical and gravimetric framework. The objectives are to: (a) characterize the main physicochemical properties and metal concentrations; (b) assess contamination levels and potential ecological risk using established geochemical indices; and (c) examine the spatial consistency between surface geochemical anomalies and deep structural features inferred from residual gravity data. By combining environmental geochemistry with indirect structural analysis, this work provides new insights into the relative roles of surficial versus deep controls on metal distribution in the Congo Coastal Basin.

MATERIALS AND METHODS

Sampling and laboratory analyses

A total of 18 stations were sampled along an approximately 8 km coastal transect between Moanda and Banana during the 2025 dry season (Figure 2). Geographic coordinates were recorded using a Garmin eTrex GPS (UTM/WGS84, ±3 m accuracy).

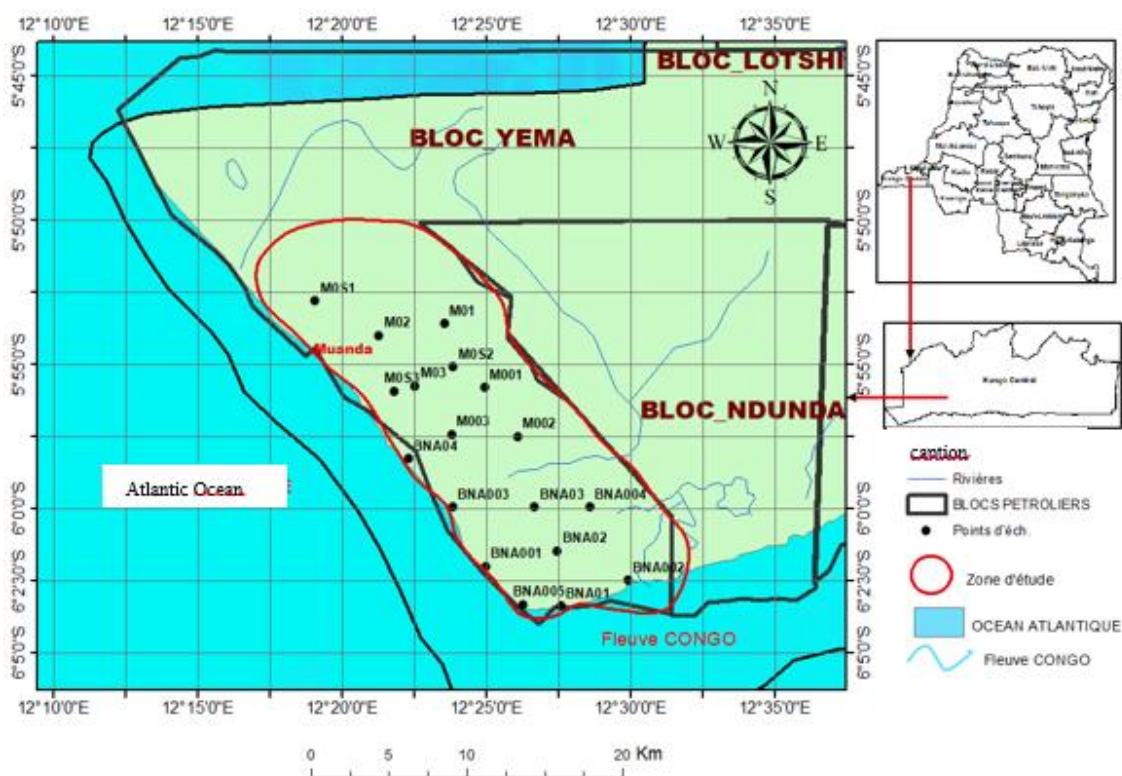


Figure 2. Location of the sampling stations.

Water content (WC) was determined by drying at 60°C, and total organic matter (TOM) was measured by loss on ignition at 550°C. Grain-size distribution was determined by laser diffraction [6]. Trace metal (TM) concentrations were measured by ICP-MS, while total mercury was analyzed using an AMA-254 analyzer. Analytical accuracy and precision were better than ±5%, and procedural blanks indicated negligible contamination [16].

Although the number of samples ($n = 18$) is relatively limited, it is comparable to several exploratory coastal studies and is sufficient to identify the dominant geochemical trends at the scale of the investigated area.

Gravimetric data

Gravimetric information was compiled from available terrestrial and marine surveys and complemented by satellite datasets (GRACE and GOCE). Residual Bouguer anomalies (Δg) were calculated to highlight subsurface density contrasts and to indirectly constrain the geometry of major deep structures (horsts, grabens and salt diapirs). This approach is used here to evaluate the spatial consistency between deep structural features and surface geochemical anomalies.

Statistical treatment and geochemical indices

Statistical analyses included Spearman rank correlations (ρ) and Principal Component Analysis (PCA) performed using XLSTAT software [1]. In this study, correlation analyses were applied not only to absolute metal concentrations but also to enrichment factors (EF) to reduce the influence of lithological background and grain-size variability. This strategy improves the identification of meaningful metal associations related to relative enrichment processes and strengthens the interpretation of dominant geochemical controls in the studied coastal environment.

Spatial distribution patterns were generated using inverse distance weighting (IDW) interpolation implemented in Surfer software. The contamination assessment relied on the following indices:

- Enrichment factor (EF) normalized to Sc and referenced to the Upper Continental Crust [20],[22]
- Geoaccumulation index (I_{geo}) [21]
- Contamination factor and degree of contamination [21]
- Pollution Load Index (PLI) [14]
- Ecological risk indices (Eri, RI) [14]

RESULTS AND DISCUSSION

Physico-chemical characteristics

Physico-chemical parameters show strong spatial variability between Moanda and Banana. Fine sediments from Moanda exhibit high water contents (WC) reaching 76.9% and total organic matter (TOM) up to 28.9%, whereas Banana soils remain generally poor in moisture (<10%) and are dominated by the sandy fraction (>80%) as is indicated in Table 1. These contrasts reflect low-energy estuarine environments versus well-drained sandy settings and confirm the key role of fine-grained fractions in trace metal retention [7],[19]. Similar controls exerted by sediment texture and depositional conditions on metal distribution have been widely documented in aquatic environments [18].

Table 1. Sampling location and composition of the samples from Moanda (M) and Banana (BNA) areas.

Sample	Sample type	Coordinates	WC	TOM	CLAY	SILT	SAND
M01	Soil	12° 19.08' E 5° 52.80' S	8.6	2.7	1.2	26.3	72.5
M02	Soil	12° 23.58' E 5° 53.58' S	7.7	2.7	2.1	45.8	52.1
M03	Soil	12° 23.88' E 5° 55.08' S	6.9	3.4	2.0	21.1	77.0
M0S1	Soil	12° 33.00' E 5° 54.00' S	32.0	8.2	1.8	28.6	69.6
M0S2	Sediment	12° 21.84' E 5° 55.92' S	76.9	28.9	0.8	70.4	28.8
M0S3	Sediment	12° 22.56' E 5° 55.74' S	49.3	13.4	3.4	69.3	27.3
M001	Sediment	12° 24.96' E 5° 55.80' S	10.2	1.6	1.4	10.0	88.6
M002	Soil	12° 26.10' E 5° 57.48' S	4.4	1.4	1.0	10.0	89.1
M003	Soil	12° 23.82' E 5° 57.42' S	5.2	3.2	1.2	9.4	89.4
BNA01	Soil	12° 25.02' E 6° 1.98' S	7.0	2.6	0.3	16.9	82.8
BNA02	Soil	12° 27.60' E 6° 3.36' S	9.0	1.7	0.7	9.2	90.0
BNA03	Soil	12° 29.94' E 6° 2.46' S	4.5	0.9	0.3	5.4	94.2
BNA04	Soil	12° 27.48' E 6° 2.46' S	5.6	0.9	0.3	4.7	95.0
BNA001	Soil	12° 23.88' E 5° 59.94' S	8.2	7.7	0.9	21.5	77.6
BNA002	Soil	12° 26.10' E 5° 59.94' S	5.8	2.1	0.9	12.4	86.7
BNA003	Soil	12° 28.62' E 5° 59.94' S	6.3	1.3	0.4	6.5	93.1
BNA004	Soil	12° 22.32' E 5° 58.26' S	2.5	1.4	0.8	13.8	85.4
BNA005	Soil	12° 26.28' E 6° 3.30' S	3.0	1.3	0.7	6.5	92.9

Metal concentrations and spatial distribution

TME concentrations show marked spatial heterogeneity (Figures 3 and 4) and maximum values reach the following:

- Zn: 412.6 mg·kg⁻¹
- Pb: 196.7 mg·kg⁻¹
- Cu: 84.2 mg·kg⁻¹

All were recorded at station M0S2, confirming the occurrence of localized metal anomalies in fine-grained sediments. The spatial distribution highlights a preferential concentration of metals in the estuarine environments of Moanda, consistent with the high adsorption capacity of fine particles and organic matter [2],[7].

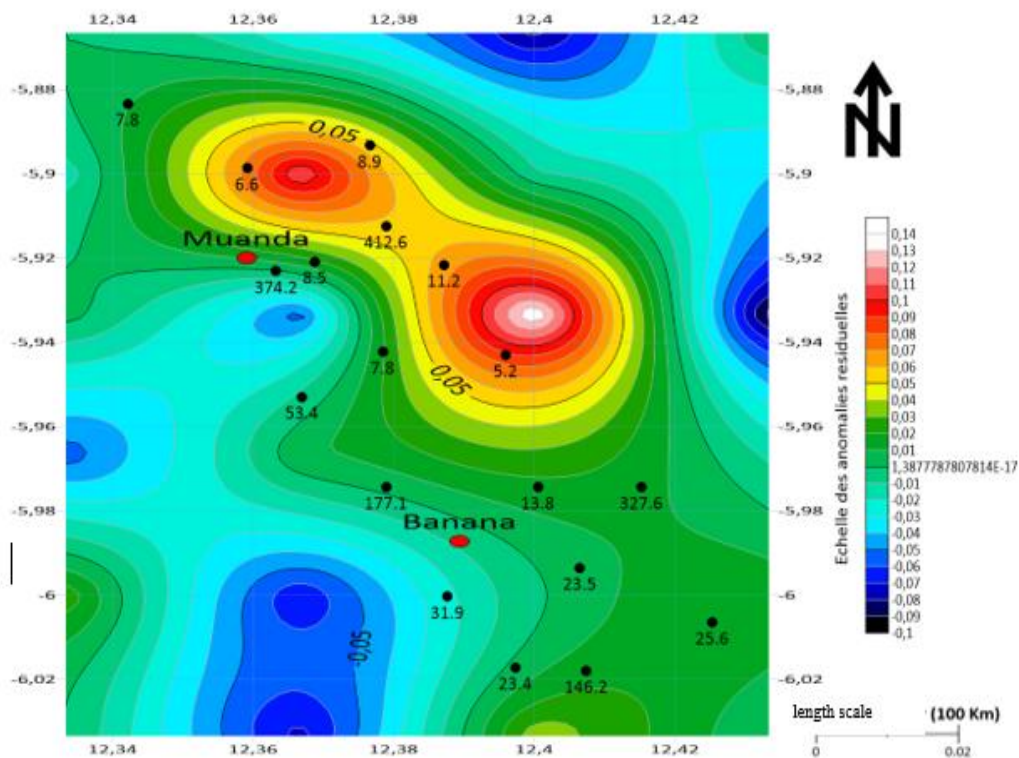


Figure 3. Spatial distribution map of zinc (Zn) in soils and sediments of the Moanda-Banana area (Surfer 20 software).

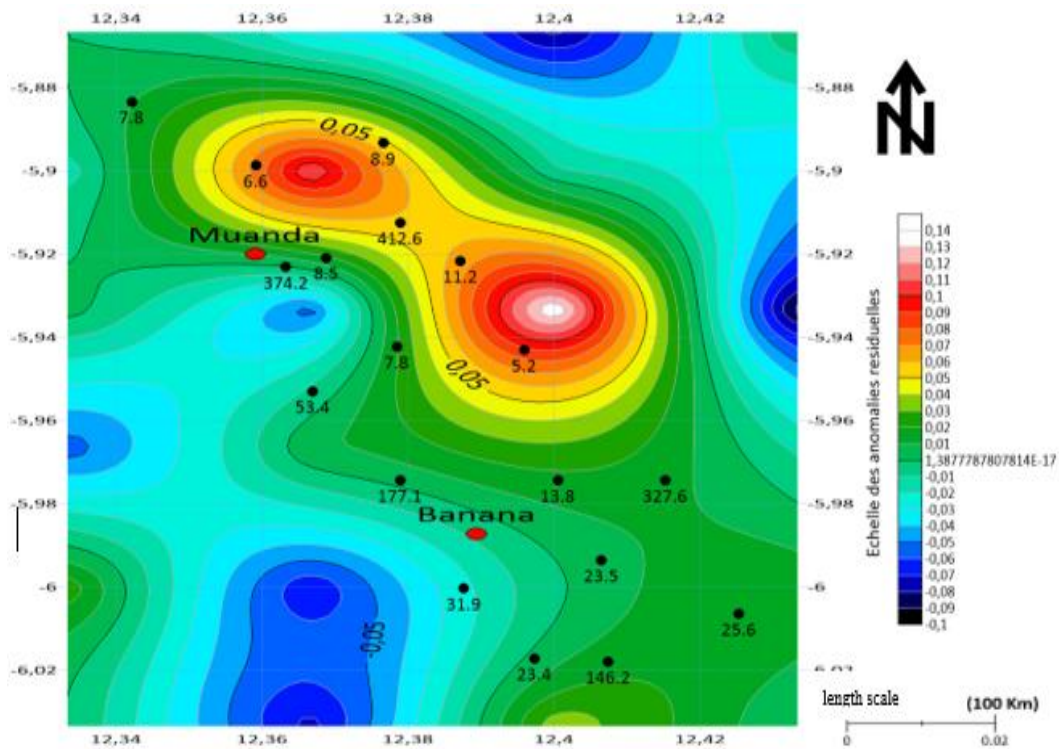


Figure 4. Spatial distribution map of lead (Pb) in soils and sediments of the Moanda-Banana area (Surfer 20 software).

Comparison with guideline thresholds

Zn frequently exceeds the SQG value ($123 \text{ mg}\cdot\text{kg}^{-1}$) and locally surpasses the PEL ($315 \text{ mg}\cdot\text{kg}^{-1}$) at station BNA004. Pb locally exceeds the PEL ($91 \text{ mg}\cdot\text{kg}^{-1}$) at stations M0S2 and M0S3. These exceedances remain spatially limited.

Geochemical indices and ecological risk

The indices indicate an overall low to moderate contamination level with localized anomalies. Comparable ecological risk patterns characterized by localized hotspots have been reported in mangrove and estuarine environments [23].

- The highest EF values are observed for Pb at stations M0S2 and M0S3.
- Igeo predominantly indicates unpolluted to moderately polluted sediments.
- Global indices (DC, PLI) confirm the presence of localized critical zones.

Similar geochemical behavior of trace metals in riverine and estuarine sediments has been widely reported in previous studies [25]. The highest RI values are recorded at M0S2 and M0S3, mainly driven by Hg and Cd, which are recognized for their high toxicity [11],[15].

Structural control

Residual gravimetric anomalies (-0.69 to $+1.97 \text{ mGal}$) reveal basement heterogeneity (Figures 5-8). The observed gravity pattern is consistent with the known structural framework of the Congo Coastal Basin, which is characterized by significant halokinetic and tectono-sedimentary heterogeneity [22]. The spatial coincidence between some positive anomalies and enriched zones (Figures 6-8) suggests a possible structural control consistent with the influence of halokinetic structures [23],[24], without excluding the effect of surficial processes. In coastal settings affected by hydrocarbon exploitation, anthropogenic inputs may locally enhance metal concentrations, although their influence often remains subordinate to sedimentary controls [9],[10].

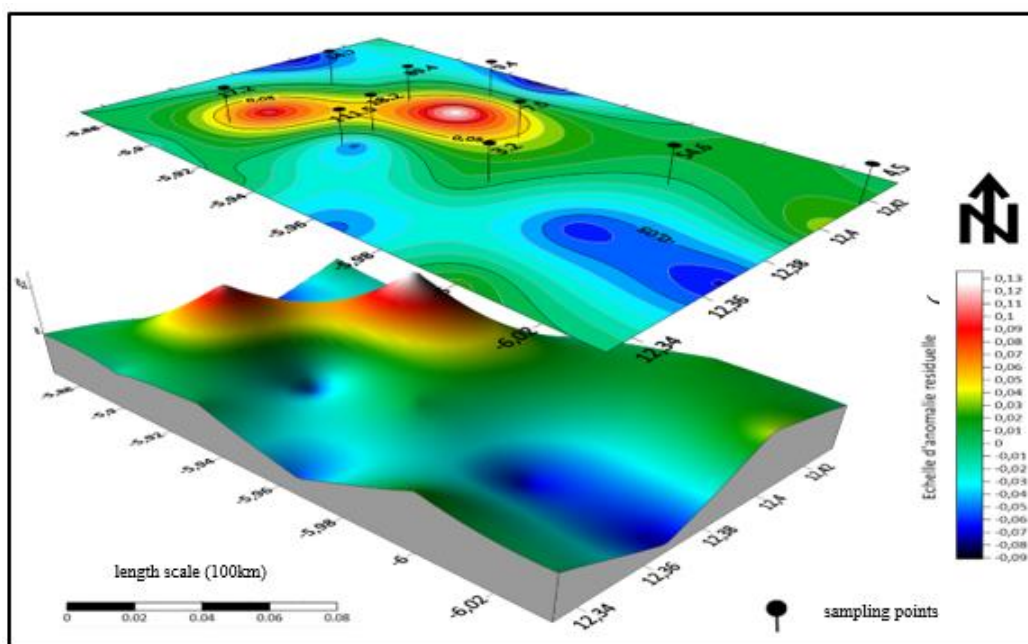


Figure 5. The spatial superposition shows a general correspondence between high metal anomalies and positive gravimetric anomalies.

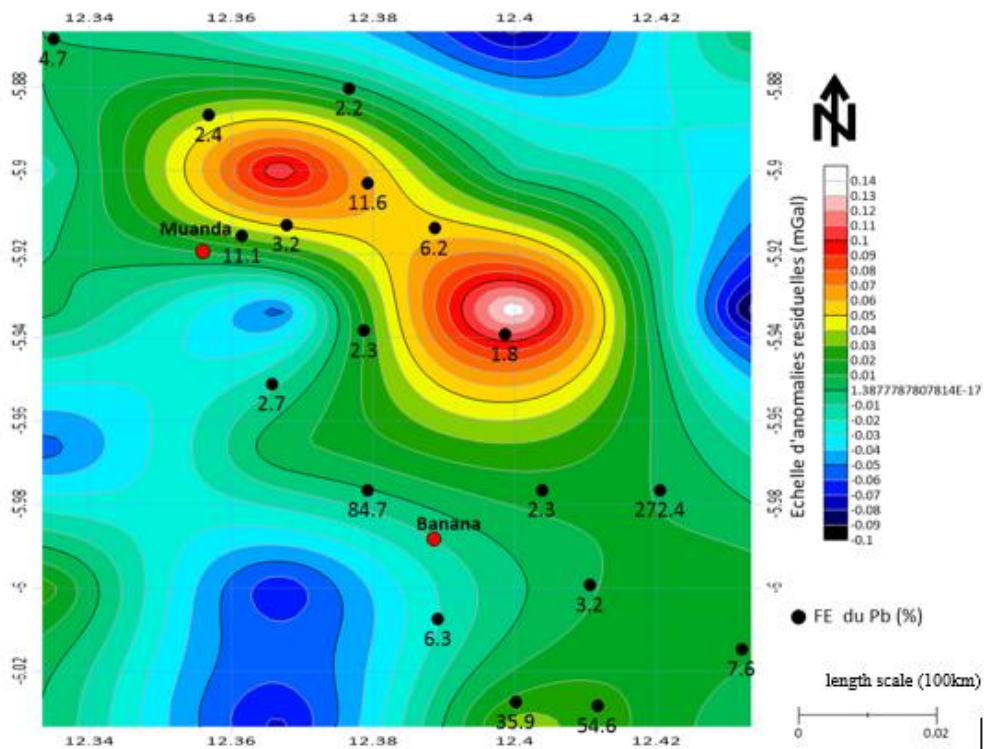


Figure 6. Spatial distribution map of the lead enrichment factor (EF-Pb) overlain on residual gravimetric anomalies (Δg) in the Moanda-Banana area.

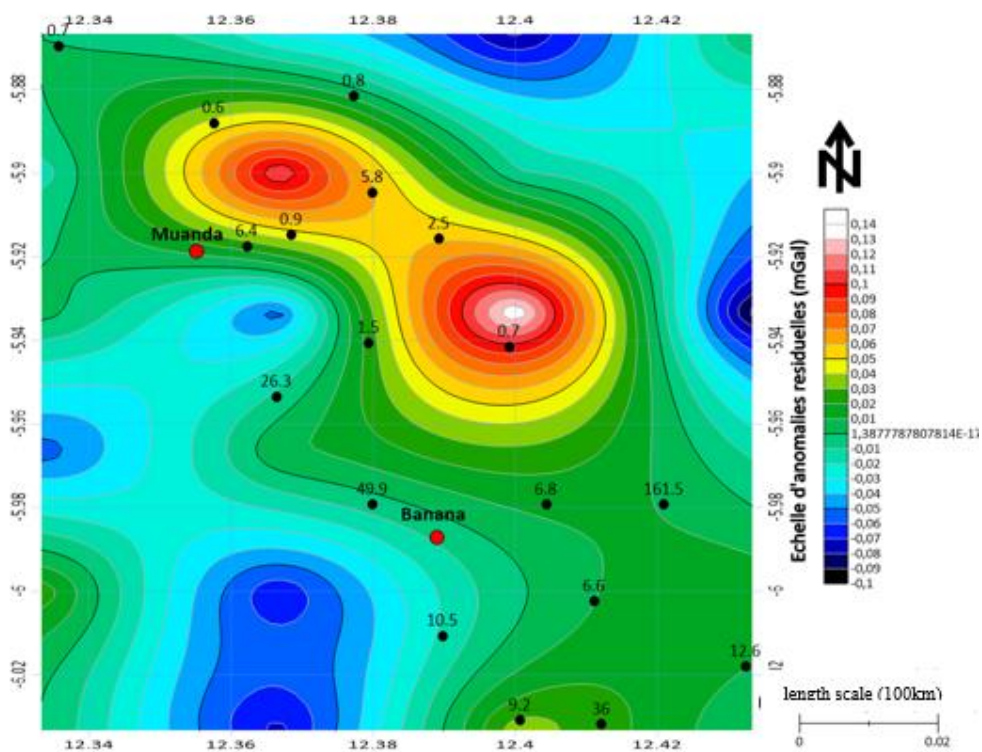


Figure 7. Spatial distribution of the zinc enrichment factor (EF-Zn) superimposed on residual gravimetric anomalies (Δg) in the Moanda-Banana area.

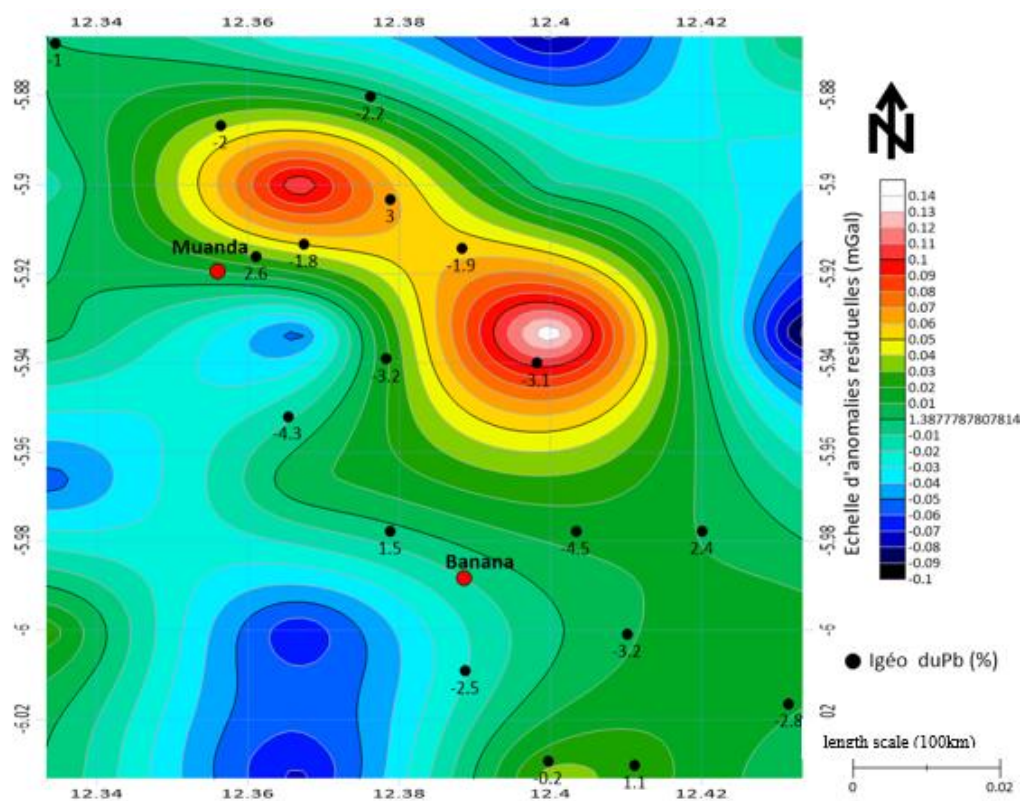


Figure 8. Spatial distribution map of the lead geoaccumulation index (I_{geo-Pb}) superimposed on residual gravimetric anomalies (Δg) in the Moanda-Banana area, illustrating the relative distribution of pollution levels in relation to deep structures.

The observed spatial correspondence should therefore be regarded as indicative rather than conclusive, since gravimetric data alone cannot provide a unique geological interpretation. Taken together, the results suggest that the geochemical behaviour of the Moanda-Banana coastal system is predominantly controlled by surficial sedimentary processes, whereas deep geogenic influences remain subordinate but locally plausible. This integrated perspective helps to avoid oversimplified interpretations that are still frequently encountered in complex coastal settings.

Multivariate analysis and Spearman correlation

Principal Component Analysis (PCA) highlights a clear structuring of the geochemical signal. The first two factorial axes alone explain 88.91% of the total variance ($F1=74.73\%$; $F2=14.19\%$), indicating a robust organization of the dataset. As illustrated by the correlation circle (Figure 9), axis F1 is mainly driven by Cu, Zn, and Pb, revealing a coherent multi-metal association. This configuration suggests the existence of common retention mechanisms or similar sources controlling the distribution of these elements.

To refine the interpretation of relationships between variables, a Spearman correlation matrix (ρ) was calculated for all studied parameters ($n = 18$; $p < 0.05$) (Table 2). Significant coefficients ($|\rho| \geq 0.50$) highlight several structuring trends in sedimentary functioning. Spearman's rank correlation coefficients (ρ) were calculated using XLSTAT software. Strong relationships are considered for $|\rho| \geq 0.50$ at $p < 0.05$.

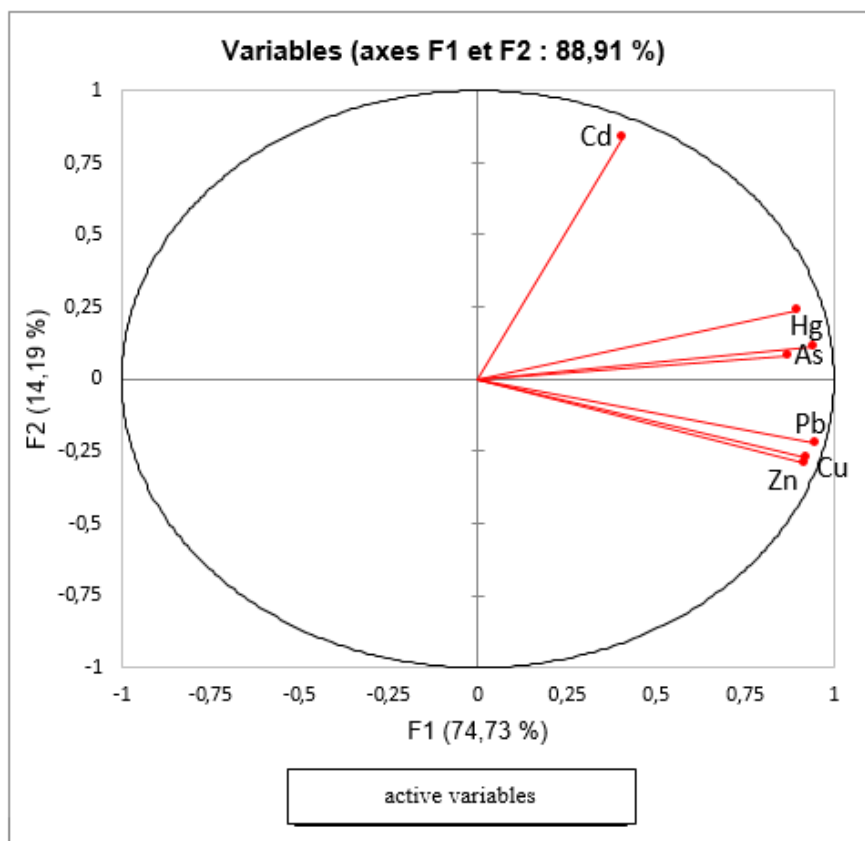


Figure 9. PCA correlation circle (F1 × F2) applied to trace metal elements.

Table 2. Spearman correlation matrix between grain size, physico-chemical parameters, and geochemical indices (EF and PLI).

Variables	EF_Cu	EF_Zn	E_Pb	EF_As	EF_Cd	EF_Hg	PLI	WC	TMO	Clay	Silt	Sand
EF_Cu	1	0.713	0.801	0.361	0.169	0.171	0.627	0.089	-0.089	-0.367	-0.269	0.285
EF_Zn	0.713	1	0.691	0.720	-0.174	-0.066	0.186	-0.282	-0.411	-0.717	-0.464	0.491
EF_Pb	0.801	0.691	1	0.362	0.137	0.271	0.764	0.182	-0.077	-0.433	-0.203	0.214
EF_As	0.361	0.720	0.362	1	-0.237	-0.289	-0.198	-0.666	-0.625	-0.701	-0.626	0.638
EF_Cd	0.169	-0.174	0.137	-0.237	1	0.433	0.457	0.166	0.079	0.279	0.162	-0.187
EF_Hg	0.171	-0.066	0.271	-0.289	0.433	1	0.545	0.289	0.451	0.138	0.386	-0.382
PLI	0.627	0.186	0.764	-0.198	0.457	0.545	1	0.544	0.334	0.106	0.232	-0.230
WC	0.089	-0.282	0.182	-0.666	0.166	0.289	0.544	1	0.710	0.422	0.656	-0.653
TMO	-0.089	-0.411	-0.077	-0.625	0.079	0.451	0.334	0.710	1	0.651	0.876	-0.873
Clay	-0.367	-0.717	-0.433	-0.701	0.279	0.138	0.106	0.422	0.651	1	0.655	-0.694
Silt	-0.269	-0.464	-0.203	-0.626	0.162	0.386	0.232	0.656	0.876	0.655	1	-0.995
Sand	0.285	0.491	0.214	0.638	-0.187	-0.382	-0.230	-0.653	-0.873	-0.694	-0.995	1

CONCLUSIONS

The present study aimed to clarify the mechanisms controlling the distribution of trace metals (TMs) in soils and sediments of the Moanda-Banana coastal zone by combining geochemical, statistical, and gravimetric approaches. The integrated framework adopted provides a more nuanced understanding of the geochemical functioning of this segment of the Congo Coastal Basin. The results reveal marked spatial variability in metal concentrations, primarily governed by surficial sedimentary characteristics. The highest enrichments are systematically associated with fine-grained sediments rich in organic matter, confirming the key role of grain size and total organic matter (TOM) in metal adsorption, complexation, and retention processes in estuarine environments. This pattern is further supported by statistical correlations and by the Cu-Zn-Pb multi-metal structure highlighted by PCA.

From an environmental perspective, geochemical indices (EF, Igeo, PLI) indicate an overall low to moderate contamination level at the regional scale, although localized anomalies are observed, particularly at stations M0S2, M0S3, and BNA004. The potential ecological risk remains generally limited; however, Hg and Cd, and locally As, constitute the main contributors to the highest risk levels due to their higher toxic-response factors. These results suggest localized ecotoxicological pressure rather than widespread degradation of the coastal system.

Multivariate analysis confirms the coherence of the multi-element signal and emphasizes the predominant role of surficial physicochemical processes in controlling TME distribution. Nevertheless, the partial spatial overlap between certain geochemical anomalies and positive gravimetric anomalies suggests that a deep structural control compatible with the halokinetic context of the Congo Coastal Basin cannot be entirely ruled out. This relationship remains indicative and should be interpreted with caution, as gravimetric data do not provide a unique solution. Overall, the study demonstrates that the geochemical functioning of the Moanda-Banana area is mainly governed by surficial sedimentary conditions, while deep geogenic influences appear secondary but locally plausible. This integrated interpretation helps avoid overly simplistic conclusions that are still common in complex coastal environments. Finally, the results highlight the value of coupling environmental geochemistry with geophysical approaches to improve the discrimination between anthropogenic signatures and natural controls in tropical passive margins. Further high-resolution investigations, combined with geochemical tracers specific to deep fluids, would help better constrain the actual role of halokinetic structures in the genesis of surface metal anomalies.

REFERENCES

- [1] Addinsoft, XLSTAT statistical and data analysis software, Addinsoft, Paris, France, 2020.
- [2] Alloway B.J., Heavy Metals in Soils, 2nd ed., Blackie Academic & Professional, London, 1995.
- [3] Alloway B.J. (Ed.), Trace Metals and Metalloids in Soils and their Bioavailability, 3rd ed., Springer, Dordrecht, 2012.
- [4] Atibu E.K., Analyses physico-chimiques et géochimiques des sols et sédiments en milieu urbain congolais, PhD Thesis, University of Kinshasa, Democratic Republic of Congo, 2021.
- [5] Atibu E.K. et al., Assessment of heavy metal contamination from abandoned mines in Kolwezi area (DRC), Chemosphere, vol. 191, pp. 1008–1020, 2018.

- [6] Blott S.J., Pye K., GRADISTAT: A grain size distribution and statistics package for the analysis of unconsolidated sediments, *Earth Surface Processes and Landforms*, vol. 26, pp. 1237–1248, 2001.
- [7] Bradl H.B., Adsorption of heavy metals on soils and soil constituents, *Journal of Soil Science and Plant Nutrition*, vol. 4, pp. 1–20, 2004.
- [8] CCME, Canadian Sediment Quality Guidelines for the Protection of Aquatic Life, Canadian Council of Ministers of the Environment, Winnipeg, 1999.
- [9] Cheyns K. et al., Cobalt exposure and environmental contamination in Katanga, *Science of the Total Environment*, vol. 490, pp. 313–321, 2014.
- [10] Eisler R., *Handbook of Chemical Risk Assessment: Metals*, CRC Press, Boca Raton, 2000.
- [11] Feng H. et al., Heavy metals in intertidal sediments of the Yangtze Estuary, *Marine Pollution Bulletin*, vol. 49, pp. 910–915, 2004.
- [12] Guo H., Zhang Y., Li X., Ecological risk of heavy metals in sediments, *Environmental Monitoring and Assessment*, vol. 110, pp. 185–202, 2005.
- [13] Håkanson L., An ecological risk index for aquatic pollution control: a sedimentological approach, *Water Research*, vol. 14, pp. 975–1001, 1980.
- [14] Jatiault R., Émanations naturelles d’hydrocarbures lourds dans le bassin du Bas-Congo, PhD Thesis, University of Perpignan, France, 2017.
- [15] Kayembe J.M. et al., Heavy metals in sediments from Kinshasa rivers, *Journal of African Earth Sciences*, vol. 147, pp. 536–543, 2018.
- [16] MacDonald D.D., Ingersoll C.G., Berger T.A., Development and evaluation of consensus-based sediment quality guidelines, *Archives of Environmental Contamination and Toxicology*, vol. 39, pp. 20–31, 2000.
- [17] McLennan S.M., Relationships between sedimentary rocks and the upper continental crust, *Geochemistry, Geophysics, Geosystems*, vol. 2, article 1021, 2001.
- [18] Müller G., Index of geoaccumulation in sediments of the Rhine River, *GeoJournal*, vol. 2, pp. 108–118, 1969.
- [19] Poté J. et al., Contaminants in Lake Geneva sediments, *Bioresource Technology*, vol. 99, pp. 7122–7131, 2008.
- [20] Taylor S.R., McLennan S.M., *The Continental Crust: Its Composition and Evolution*, Blackwell Scientific Publications, Oxford, 1985.
- [21] Yin X. et al., Heavy metal enrichment as hydrocarbon seepage indicators in marine sediments, *Marine and Petroleum Geology*, vol. 73, pp. 1–12, 2016.
- [22] Gaffney, Cline & Associates, Étude sur les réserves du bassin côtier: aspects géologiques régionaux et prospects d’exploration, Technical Report, 51 p., 1988.
- [23] CONOCO, Étude de la zone rendue du bassin côtier, Internal Technical Report, 1990.
- [24] Förstner U., Wittmann G.T.W., *Metal Pollution in the Aquatic Environment*, Springer, Berlin, 1983.
- [25] Sakan S.M. et al., Heavy metals in river sediments: sources, distribution and risk assessment, *Journal of Environmental Management*, vol. 90, pp. 3382–3390, 2009.

APPENDIX A

A1. Concentrations of trace metal elements in soil and sediment samples

Table A1. Concentrations of trace metal elements in soil and sediment samples ($\text{mg}\cdot\text{kg}^{-1}$).

Sample	Cu	Zn	As	Cd	Pb	Hg
M0S1	4.3	7.8	1.5	0	13.1	0
M01	4.7	8.9	1.5	0.1	5.7	0
M0S2	84.2	412.6	15.8	0.3	196.7	1.2
M02	4.3	6.6	1.1	0	6.4	0
M0S3	70.2	374.2	5	0.3	156.3	1.2
M03	8.1	8.5	0.9	0	7.4	0
M001	6.7	11.2	0.6	0.7	6.8	0
M002	4	5.2	1.4	0	3	0
M003	4.7	7.8	0.8	0	2.8	0
BNA001	3.7	31.9	1	0	4.6	0
BNA01	44.8	146.2	0.8	0	53	0
BNA002	2.1	25.6	1	0	3.7	0
BNA02	1.7	23.5	1.1	0	2.7	0
BNA003	41.1	177.1	1.2	0	72	0
BNA03	1	13.8	0.5	0	1.1	0
BNA004	54.2	327.6	0.6	0	132.3	0
BNA04	1.4	53.4	0.6	0	1.3	0
BNA005	3	23.4	0.8	0.3	21.8	0
SQGs	35.7	123	5.9	0.6	35	0,17
PELs	197	315	17	3.5	91	0.49

A2. Geochemical indices

Table A2. Enrichment factors (EF) of trace metals (TMs) in soil and sediment samples from the Moanda-Banana coastal area.

Sample	EF-Cu	EF-Zn	EF-Pb	EF-As	EF-Cd	EF-Hg
M0S1	1.0	0.7	4.7	6.1	0.0	0.0
M01	1.3	0.8	2.2	6.7	6.8	0.0
M0S2	3.4	5.8	11.6	10.5	3.1	24.0
M02	1.1	0.6	2.4	4.7	0.0	0.0
M0S3	3.4	6.4	11.1	4.0	3.7	29.0
M03	2.4	0.9	3.2	4.4	0.0	0.0
M001	4.2	2.5	6.2	6.2	111.1	0.0
M002	1.6	0.7	1.8	9.3	0.0	0.0
M003	2.6	1.5	2.3	7.5	0.0	0.0

BNA001	3.5	10.5	6.3	15.6	0.0	0.0
BNA01	31.4	36.0	54.6	9.3	0.0	0.0
BNA002	2.9	12.6	7.6	23.3	0.0	0.0
BNA02	1.4	6.6	3.2	14.7	0.0	0.0
BNA003	32.9	49.9	84.7	16.0	0.0	0.0
BNA03	1.4	6.8	2.3	11.7	0.0	0.0
BNA004	75.9	161.5	272.4	14.0	0.0	0.0
BNA04	2.0	26.3	2.7	14.0	0.0	0.0
BNA005	3.4	9.2	35.9	14.9	85.7	0.0
FE < 1	Background /No enrichment					
1 ≤ FE < 3	Minor enrichment					
3 ≤ FE < 5	Moderate enrichment					
5 ≤ FE < 10	Significant					
FE ≥ 10	Severe to very high enrichment					

Table A3. Geoaccumulation index (Igeo) of trace metal elements in soils and sediments of the Moanda-Banana area.

Sample	Igeo-Cu	Igeo-Zn	Igeo-Pb	Igeo-As	Igeo-Cd	Igeo-Hg
M0S1	-3.1	-3.8	-1.0	-0.6	-	-
M01	-3.0	-3.6	-2.2	-0.6	-0.6	-
M0S2	1.2	2.0	3.0	2.8	1.0	4.0
M02	-3.1	-4.0	-2.0	-1.0	-	-
M0S3	0.9	1.8	2.6	1.2	1.0	4.0
M03	-2.2	-3.7	-1.8	-1.3	-	-
M001	-2.5	-3.3	-1.9	-1.9	2.2	-
M002	-3.2	-4.4	-3.1	-0.7	-	-
M003	-3.0	-3.8	-3.2	-1.5	-	-
BNA001	-3.3	-1.7	-2.5	-1.2	-	-
BNA01	0.3	0.5	1.1	-1.5	-	-
BNA002	-4.2	-2.1	-2.8	-1.2	-	-
BNA02	-4.5	-2.2	-3.2	-1.0	-	-
BNA003	0.1	0.7	1.5	-0.9	-	-
BNA03	-5.2	-3.0	-4.5	-2.2	-	-
BNA004	0.5	1.6	2.4	-1.9	-	-
BNA04	-4.7	-1.0	-4.3	-1.9	-	-
BNA005	-3.6	-2.2	-0.2	-1.5	1.0	-
Igeo ≤ 0	Unpolluted					
0 < Igeo ≤ 1	Slightly polluted					
1 < Igeo ≤ 2	Moderately polluted					
2 < Igeo ≤ 3	Strongly polluted					
Igeo > 3	Very strongly polluted					

A4. Global contamination indices (CF, DC, DCm and PLI)

Table A4. Contamination factor (CF), degree of contamination (DC), modified degree of contamination (DCm), and pollution load index (PLI) for soils and sediments of the Moanda-Banana area.

Sample	CF_Cu	FC_Zn	FC_Pb	FC_As	FC_Cd	FC_Hg	DC	DCm	PLI
M0S1	0.2	0.1	0.8	1.0	0.0	0.0	63.2	9.0	1.0
M01	0.2	0.1	0.3	1.0	1.0	0.0	39.3	5.6	0.8
M0S2	3.4	5.8	11.6	10.5	3.0	24.0	273.8	39.1	12.0
M02	0.2	0.1	0.4	0.7	0.0	0.0	55.8	8.0	0.7
M0S3	2.8	5.3	9.2	3.3	3.0	24.0	249.8	35.7	9.4
M03	0.3	0.1	0.4	1.0	0.0	0.0	68.1	9.7	0.9
M001	0.3	0.1	0.4	0.9	7.0	0.0	69.3	9.9	1.2
M002	0.2	0.1	0.2	0.4	0.0	0.0	51.3	7.3	0.6
M003	0.2	0.1	0.2	0.5	0.0	0.0	39.9	5.7	0.6
BNA001	0.1	0.4	0.3	3.1	0.0	0.0	29.3	4.2	0.8
BNA01	1.8	2.0	3.1	35.3	0.0	0.0	41.9	6.0	2.9
BNA002	0.1	0.4	0.2	2.5	0.0	0.0	18.0	2.6	0.6
BNA02	0.1	0.3	0.1	1.8	0.0	0.0	22.4	3.2	0.6
BNA003	1.6	2.5	4.2	48.0	0.0	0.0	22.5	3.2	2.8
BNA03	0.0	0.2	0.1	0.7	0.0	0.0	25.1	3.6	0.3
BNA004	2.2	4.6	7.8	88.2	0.0	0.0	33.8	4.8	3.6
BNA04	0.0	0.7	0.1	0.9	0.0	0.0	10.2	1.4	0.4
BNA005	0.1	0.3	1.3	14.5	3.0	0.0	27.5	3.9	1.1

CF		DC	
CF < 1	Low contamination	DC < 6	Low degree of contamination
1 ≤ CF < 3	Moderate contamination	6 ≤ DC < 12	Moderate degree of contamination
3 ≤ CF < 6	Considerable contamination	12 ≤ DC < 24	Considerable degree of contamination
CF ≥ 6	Very high contamination	DC ≥ 24	Very high degree of contamination

DCm		PLI	
DCm < 1.5	Low degree of contamination	PLI = 1	No pollution
1.5 ≤ DCm < 2	Moderate degree of contamination	1 < PLI ≤ 1.5	Low to moderate pollution
2 ≤ DCm < 4	Considerable degree of contamination	1.5 < PLI ≤ 2	Significant pollution
DCm ≥ 4	Very high degree of contamination	2 < PLI ≤ 3	High pollution
		PLI > 3	Very High pollution

A5. Ecological risk indices (Eri and RI)

Table A5. Ecological risk factor (Eri) and potential ecological risk index (RI)
for soils and sediments of the Moanda-Banana area.

Sample	Eri_Cu	Eri_Zn	Eri_Pb	Eri_As	Eri_Cd	Eri_Hg	RI
M0S1	1.0	0.1	4.0	10.0	0.0	0.0	15.1
M01	1.0	0.1	1.5	10.0	30.0	0.0	42.6
M0S2	17.0	5.8	58.0	105.0	90.0	960.0	1235.8
M02	1.0	0.1	2.0	7.0	0.0	0.0	10.1
M0S3	14.0	5.3	46.0	33.0	90.0	960.0	1148.3
M03	1.5	0.1	2.0	10.0	0.0	0.0	13.6
M001	1.5	0.1	2.0	9.0	210.0	0.0	222.6
M002	1.0	0.1	1.0	4.0	0.0	0.0	6.1
M003	1.0	0.1	1.0	5.0	0.0	0.0	7.1
BNA001	0.5	0.4	1.5	31.0	0.0	0.0	33.4
BNA01	9.0	2.0	15.5	353.0	0.0	0.0	379.5
BNA002	0.5	0.4	1.0	25.0	0.0	0.0	26.9
BNA02	0.5	0.3	0.5	18.0	0.0	0.0	19.3
BNA003	8.0	2.5	21.0	480.0	0.0	0.0	511.5
BNA03	0.0	0.2	0.5	7.0	0.0	0.0	7.7
BNA004	11.0	4.6	39.0	882.0	0.0	0.0	936.6
BNA04	0.0	0.7	0.5	9.0	0.0	0.0	10.2
BNA005	0.5	0.3	6.5	145.0	90.0	0.0	242.3
Eri < 40 / RI < 150			Low ecological risk				
40 ≤ Eri < 80 / 150 ≤ RI < 300			Moderate ecological risk				
80 ≤ Eri < 160 / 300 ≤ RI < 600			Considerable ecological risk				
160 ≤ Eri < 320 / 600 ≤ RI < 1200			High ecological risk				
Eri ≥ 320 / RI ≥ 1200			Very high ecological risk				

Received: February 2026; Revised: March 2026; Accepted: March 2026; Published: March 2026